Table 2 Results of 93 patients treated with radiologic embolotherapy for gastric varices *n* (%)

Results	BRTO	PTO	Com-T	Total
Complete disappearance of gastric varices	75	8	10	93
Variceal rebleeding	1 (1)	1 (13)	0	2 (2)
Recurrence of gastric varices	3 (4)	3 (38)	0	6 (7)
Aggravation of esophageal varices	27 (36)	3 (38)	3 (30)	33 (36)
Death	21 (28)	0	2 (30)	23 (25)
Cause of death				
Hepatic failure	8 (11)	0	1 (10)	9 (10)
Hepatocellular carcinoma	8 (11)	0	0	8 (9)
Cerebral hemorrhage	2 (3)	0	0	2 (2)
Renal failure	2 (3)	0	0	2 (2)
Pneumonia	1 (1)	0	0	1 (1)
Psychosis	0	0	1 (10)	1 (1)

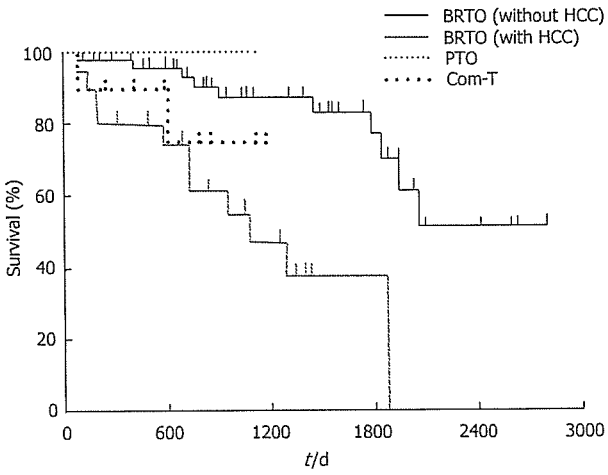

Figure 3 Cumulative survivals after radiologic embolotherapy for gastric varices.

7 (9%) patients who showed no improvement in the gastric varices, as indicated by CT, underwent an additional BRTO procedure. The BRTO procedure was performed twice on 5 patients, and three times on 2 patients with large gastric varices and dilated collateral veins. The overall BRTO technical success rate was 89% (68/75 + 5/7 + 2/2 = 75/84). In 18 patients who underwent variceal embolization by PTO alone or combined with BRTO, CT examination revealed that total obliteration of the gastric varices was achieved in all patients 1 wk after the initial procedure. According to the definition of technical success, the success rate was 91%, 100% and 100% in the BRTO, PTO and combined therapy.

During the follow-up period, recurrence of gastric varices was found in 3 patients (4%) in the BRTO group (1939, 1067, and 723 d after the BRTO procedure) and in 3 patients (38%) in the PTO group (1123, 574, and 150 d after the PTO procedure). In 3 patients in the BRTO group, the GOV2 type of recurrent gastric varices occurred after treatment of IGV1 with the BRTO procedure. Among the 3 patients in the PTO group, 2 had gastric varices of the GOV2 type, while 1 had gastric varices of the IGV1 type before the PTO procedure. In these 3 patients, the type of recurrent gastric varices was identical to those found prior to the PTO treatment. These recurrent gastric varices were strictly followed up without additional treatment. No variceal recurrence was found in the combined therapy group (Table 2).

Rebleeding was observed in 2 patients after treatment (1 patient had received the BRTO procedure and the other had received the PTO treatment). In 1 patient in the BRTO group, rebleeding from gastric varices was observed before the additional BRTO procedure because of incomplete obliteration of the varices by the initial treatment. The gastric varices of the patient were obliterated by the second BRTO procedure. In 1 of the 3 patients who had been noted to have recurrent gastric varices in the PTO group, the rebleeding occurred due to the recurrence. The patient refused additional interventional embolotherapy and underwent Hassab's devascularization after initial hemostasis by an endoscopic procedure[16]. In the combined group, no rebleeding was found.

After the BRTO procedure, the 1- and 3-year survival rates were 92% and 75%, respectively. The 1- and 3-year survival rates were 98% and 87% in the patients without HCC in the BRTO group, 100% and 100% in the PTO group, and 90% and 75% in the combined therapy group, respectively. There was no significant difference across the three groups. On the other hand, the 1- and 3-year survival rates were 80% and 47% in the patients with HCC in the BRTO group. The survival rate after the BRTO procedure was significantly higher in the patients without HCC than in those with HCC ($P < 0.01$, Figure 3).

During the follow-up period, 21 patients in the BRTO group and 2 patients in the combined therapy group died; however, no patients in the PTO group died. Death due to hepatic failure occurred in the case of 8 (11%) patients in the BRTO group (range, 91-2056 d; median, 743 d) and 1 (10%) patient in the combined therapy group (605 d after the procedure). No significant difference was observed among the three procedures. The other causes of death in the BRTO group were hepatocellular carcinoma, cerebral hemorrhage, renal failure (due to diabetes mellitus), and pneumonia. In the combined therapy group, 1 patient died from psychosis 83 d after the procedure (Table 2).

All three procedures caused adverse effects, such as fever (> 38.0℃), hemoglobinuria, abdominal pain, chest pain, nausea, and blood pressure elevation. On the other hand, ascites, pleural effusion, headache, and hepatic encephalopathy were detected in the BRTO group. No fatal complications were observed (Table 3). We have reported the change in the hepatic and renal function tests in patients treated with the BRTO procedure[17]. In terms of laboratory data, there was no difference in the three procedures. The esophageal varices aggravated in 27 (36%) patients in the BRTO group and in 3 patients

Table 3 Complication of treatment *n* (%)

Complication	BRTO	PTO	Com-T	Total
Fever	47 (63)	4 (50)	9 (90)	60 (65)
Hemoglobinuria	35 (47)	3 (38)	10 (100)	48 (52)
Abdominal pain	48 (64)	6 (75)	7 (70)	66 (71)
Nausea	31 (41)	4 (50)	6 (60)	41 (44)
Blood pressure elevation[1]	22 (29)	2 (25)	4 (40)	28 (30)
Ascites	3 (4)	0	0	3 (3)
Pleural effusion	5 (7)	0	0	5 (5)
Headache	6 (8)	0	0	6 (7)
Hepatic encephalopathy	1 (1)	0	0	1 (1)
Chest pain	24 (32)	2 (25)	7 (70)	33 (36)

[1]More than 20 mmHg elevation.

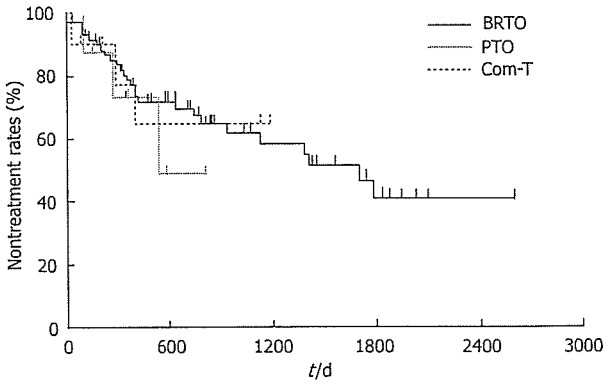

Figure 4 Cumulative non-treatment rates for esophageal varices after radiologic embolotherapy.

in each of the PTO (38%) and combined therapy groups (33%). These were treated using the usual methods of EVL and EIS. During the course after the procedures, the cumulative nontreatment rates of esophageal varices at 1 year were 79%, 73%, and 77% in the BRTO, PTO, and combined therapy groups, respectively. There was no significant difference in the three procedures (Figure 4). The nontreatment rates of esophageal varices in the BRTO group at 1 and 3 year were 61% and 42% in the patients with esophageal varices and 86% and 70% in the patients without them prior to BRTO, respectively. The cumulative nontreatment rates of esophageal varices in the BRTO group were significantly lower in the patients with esophageal varices than in the patients without them prior to BRTO ($P < 0.01$, Figure 5).

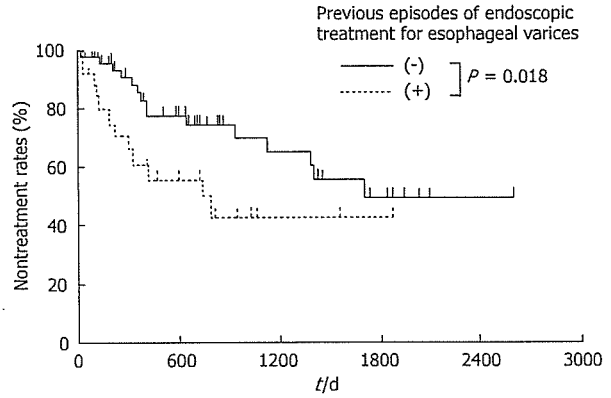

Figure 5 Cumulative non-treatment rates for esophageal varices after balloon-occluded retrograde transvenous obliteration.

DISCUSSION

Since Kanagawa *et al*[18] reported the treatment of gastric varices by BRTO with 50 g/L EOI, BRTO has been widely accepted as an interventional embolotherapy for gastric varices in Japan. Subsequently, many reports demonstrated the clinical efficacy and safety of this treatment[6-9]. According to several reports, the therapeutic result obtained by this treatment is satisfactory and the recurrence rate is very low. In our study, the BRTO procedure was angiographically successful in 81% (75/93) patients; hence, our results are consistent with those reported previously[9,10,19]. Recurrence of gastric varices was found in only 3 of the 75 patients who had undergone the BRTO procedure. In all 3 patients, the GOV2 type of recurrent gastric varices occurred after treatment of IGV1 with the BRTO procedure. Gastric varices that are classified as GOV2 have a direct connection with the coronary vein and esophageal varices. The aggravation of esophageal varices caused by damage of portal hemodynamics after the BRTO procedure has been well documented. It appeared that the mechanism of these recurrent gastric varices was similar to that observed in the aggravation of esophageal varices.

The BRTO procedure is applied to gastric varices that have a portosystemic shunt route to the inferior vena cava. Some gastric varices without a major shunt or those with many small collateral circulations are difficult to treat by the BRTO procedure. Reports of the refractory varices treated with the BRTO procedure are rare[10,20,21]. Thus, an adequate treatment strategy for refractory gastric varices has not yet been established. We performed the PTO procedure for uncontrollable gastric varices treated by the BRTO procedure. The first report on the treatment of gastric varices by the PTO procedure was described by Scott *et al* in 1976[15]. Since the previously used PTO procedure could obliterate inflow vessels but could not easily obliterate gastric varices completely, it was associated with a high incidence of rebleeding and recurrences. Our PTO procedure would fill the lumen of the gastric varices with the sclerotic agent in an antegrade manner by stopping the inflow into varices using coils and a balloon catheter that is wedged in an antegrade manner. EO, an anionic surfactant, infiltrates and destroys the cell membrane of venous endothelial cells. Damage to the venous endothelium caused by EO is greater than that caused by a 50% glucose solution. Therefore, EO causes thrombus formation in gastric varices, and gastric varices thrombosed by EO have been reported to be completely disappeared[6-9]. The PTO procedure that we used is the same as BRTO in that the gastric varices are thrombosed.

In this study, the PTO procedure rescued only 44%

(8/18) patients who had uncontrollable gastric varices treated by the BRTO procedure. To block the gastric variceal blood flow, the PTO procedure, which involves the catheterization of the only feeding vein, may be less effective than the combined therapy. It is probable that the antegrade procedure could obliterate the feeding vein but could not completely and easily obliterate the varices with a large draining vein. The patients in the PTO group had more minor collateral circulation, such as pericardial or hemiazygous veins, as compared with the patients in the BRTO group.

The indication for the PTO procedure with 50 g/dL EOI was the presence of gastric varices without large draining veins and varices untreated by BRTO because of many small collateral veins. In the PTO group, the gastric varices recurred in 3 patients with incomplete eradication; bleeding occurred in 1 of these patients. It appeared that the therapeutic efficacy of the PTO procedure was incomplete for uncontrollable gastric varices treated by the BRTO procedure.

Some of the patients who underwent attempted BRTO had no embolization performed at all *via* antegrade route because of unfavorable anatomy whilst others had some embolization with coils and/or sclerosant. We performed the combined BRTO and PTO therapy on patients in whom uncontrollable gastric varices had been treated by the BRTO procedure and the PTO procedure. Reports on the varices that had been treated with combined therapy, which obstructs both the feeding and the draining veins of the varices, are rare. Kimura *et al*[22] reported a case of rectal varices that was treated with double balloon-occluded embolotherapy in 1997. Similarly, Ota *et al*[23] reported the results of combined therapy comprising BRTO and transileocolic vein obliteration (TIO) in a patient with duodenal varices. Kiyosue *et al*[24] suggested that the indication for combined therapy was the presence of gastric varices that are supplied by single or multiple gastric veins with coexistent gastric veins that are directly contiguous with the shunt but do not contribute to the varices. However, to the best of our knowledge, there have been no studies on the treatment of gastric varices by combined BRTO and PTO therapy. In our study, the therapeutic result of the combined therapy was satisfactory. No bleeding or variceal recurrence was found in the combined therapy group.

Combined therapy, which can obstruct both the feeding and the draining veins of gastric varices to retain the sclerosing agent completely in the varices, may provide a better control of the gastric variceal blood flow than that provided by the only BRTO or PTO procedure. Our study demonstrates that combined therapy is very effective in the treatment of gastric varices, irrespective of whether patients have had a large gastrorenal shunt and/or collateral circulation. Since the combined therapy may eliminate the hemodynamics of gastric varices, this procedure may be more effective than other procedures. In fact, the obliteration of the gastric varices by this method was successful in all 10 patients in whom the BRTO or PTO procedure was unsuccessfully performed.

Although only the femoral or internal jugular vein is punctured in the BRTO procedure, the combined therapy or the PTO procedure requires a puncture in the liver. Therefore, the BRTO procedure is less invasive than the other procedures. Since the combined therapy appears to be similar to the BRTO procedure in terms of safety and efficacy, we propose that the BRTO procedure should be the first choice of the treatment for gastric varices. The combined therapy should only be performed in the case of highly selected patients. We believe that the indication for combined therapy is refractory gastric varices that remain untreated despite being subjected to the BRTO and PTO procedures. In addition, the PTO procedure is less invasive than the combined therapy, because the femoral or internal jugular vein is not punctured in this procedure. Thus, the results presented here indicate that the algorithmic strategy for treating gastric varices using the BRTO and PTO procedures and the combined therapy is feasible (Figure 1).

These three procedures for obliterating the gastric varices may increase the portal pressure. Aggravation of the esophageal by these treatments varices was recognized to be a result of elevated portal pressure. From the viewpoint of aggravation of esophageal varices, no statistical differences were demonstrated among the three procedures. However, non-treatment rate of esophageal varices after the BRTO was significantly lower in those who were treated esophageal varices before BRTO than those not treated. Our results are consistent with those reported earlier[19]. Periodic endoscopic follow-up is recommended after the eradication of gastric varices, particularly in patients with esophageal varices prior to the BRTO procedure. The mortality rate for gastric variceal bleeding is much higher than that for esophageal variceal bleeding[25]. Therefore, we believe that these changes in the portal hemodynamics were preferable because esophageal varices can be easily controlled by endoscopic therapy.

In conclusion, combined BRTO and PTO therapy may rescue cases with uncontrollable gastric fundal varices that remained even after treatment with BRTO and/or PTO. Our study could establish the algorithmic strategy for treating gastric fundal varices using interventional embolotherapy. However, there were limitations of our study, including retrospective nature and discrepancy in sample size between the BRTO, PTO and combined therapy groups. Further, long-term prospective studies would assist in clarifying the effect of combined BRTO and PTO therapy.

REFERENCES

1 **Rossle M**, Haag K, Ochs A, Sellinger M, Noldge G, Perarnau JM, Berger E, Blum U, Gabelmann A, Hauenstein K.The transjugular intrahepatic portosystemic stent-shunt procedure for variceal bleeding. *N Engl J Med* 1994; **330**: 165-171

2 **LaBerge JM**, Somberg KA, Lake JR, Gordon RL, Kerlan RK Jr, Ascher NL, Roberts JP, Simor MM, Doherty CA, Hahn J.Two-year outcome following transjugular intrahepatic portosystemic shunt for variceal bleeding: results in 90 patients. *Gastroenterology* 1995; **108**: 1143-1151

3 **Albillos A**, Ruiz del Arbol L. "Salvage" transjugular intrahepatic portosystemic shunt: gastric fundal compared with esophageal variceal bleeding. *Gastrointest Endosc* 1999; **50**: 294-295

4 **Barange K**, Peron JM, Imani K, Otal P, Payen JL, Rousseau H, Pascal JP, Joffre F, Vinel JP. Transjugular intrahepatic porto-

systemic shunt in the treatment of refractory bleeding from ruptured gastric varices. *Hepatology* 1999; **30**: 1139-1143
5 **Rees CJ**, Nylander DL, Thompson NP, Rose JD, Record CO, Hudson M. Do gastric and oesophageal varices bleed at different portal pressures and is TIPS an effective treatment? *Liver* 2000; **20**: 253-256
6 **Hirota S**, Matsumoto S, Tomita M, Sako M, Kono M. Retrograde transvenous obliteration of gastric varices. *Radiology* 1999; **211**: 349-356
7 **Fukuda T**, Hirota S, Sugimura K. Long-term results of balloon-occluded retrograde transvenous obliteration for the treatment of gastric varices and hepatic encephalopathy. *J Vasc Interv Radiol* 2001; **12**: 327-336
8 **Chikamori F**, Kuniyoshi N, Shibuya S, Takase Y. Eight years of experience with transjugular retrograde obliteration for gastric varices with gastrorenal shunts. *Surgery* 2001; **129**: 414-420
9 **Kitamoto M**, Imamura M, Kamada K, Aikata H, Kawakami Y, Matsumoto A, Kurihara Y, Kono H, Shirakawa H, Nakanishi T, Ito K, Chayama K. Balloon-occluded retrograde transvenous obliteration of gastric fundal varices with hemorrhage. *AJR Am J Roentgenol* 2002; **178**: 1167-1174
10 **Ninoi T**, Nakamura K, Kaminou T, Nishida N, Sakai Y, Kitayama T, Hamuro M, Yamada R, Arakawa T, Inoue Y. TIPS versus transcatheter sclerotherapy for gastric varices. *AJR Am J Roentgenol* 2004; **183**: 369-376
11 **Pugh RN**, Murray-Lyon IM, Dawson JL, Pietroni MC, Williams R. Transection of the oesophagus for bleeding oesophageal varices. *Br J Surg* 1973; **60**: 646-649
12 **Chikamori F**, Kuniyoshi N, Shibuya S, Takase Y. Short-term hemodynamic effects of transjugular retrograde obliteration of gastric varices with gastrorenal shunt. *Dig Surg* 2000; **17**: 332-336
13 **Sarin SK**, Lahoti D, Saxena SP, Murthy NS, Makwana UK. Prevalence, classification and natural history of gastric varices: a long-term follow-up study in 568 portal hypertension patients. *Hepatology* 1992; **16**: 1343-1349
14 **Sarin SK**, Kumar A. Gastric varices: profile, classification, and management. *Am J Gastroenterol* 1989; **84**: 1244-1249
15 **Scott J**, Dick R, Long RG, Sherlock S. Percutaneous transhepatic obliteration of gastro-oesophageal varices. *Lancet* 1976; **2**: 53-55
16 **Hassab MA**. Gastroesophageal decongestion and splenectomy in the treatment of esophageal varices in bilharzial cirrhosis: further studies with a report on 355 operations. *Surgery* 1967; **61**: 169-176
17 **Shimoda R**, Horiuchi K, Hagiwara S, Suzuki H, Yamazaki Y, Kosone T, Ichikawa T, Arai H, Yamada T, Abe T, Takagi H, Mori M. Short-term complications of retrograde transvenous obliteration of gastric varices in patients with portal hypertension: effects of obliteration of major portosystemic shunts. *Abdom Imaging* 2005; **30**: 306-313
18 **Kanagawa H**, Mima S, Kouyama H, Gotoh K, Uchida T, Okuda K. Treatment of gastric fundal varices by balloon-occluded retrograde transvenous obliteration. *J Gastroenterol Hepatol* 1996; **11**: 51-58
19 **Ninoi T**, Nishida N, Kaminou T, Sakai Y, Kitayama T, Hamuro M, Yamada R, Nakamura K, Arakawa T, Inoue Y. Balloon-occluded retrograde transvenous obliteration of gastric varices with gastrorenal shunt: long-term follow-up in 78 patients. *AJR Am J Roentgenol* 2005; **184**: 1340-1346
20 **Koito K**, Namieno T, Nagakawa T, Morita K. Balloon-occluded retrograde transvenous obliteration for gastric varices with gastrorenal or gastrocaval collaterals. *AJR Am J Roentgenol* 1996; **167**: 1317-1320
21 **Ibukuro K**, Mori K, Tsukiyama T, Inoue Y, Iwamoto Y, Tagawa K. Balloon-occluded retrograde transvenous obliteration of gastric varix draining via the left inferior phrenic vein into the left hepatic vein. *Cardiovasc Intervent Radiol* 1999; **22**: 415-417
22 **Kimura T**, Haruta I, Isobe Y, Ueno E, Toda J, Nemoto Y, Ishikawa K, Miyazono Y, Shimizu K, Yamauchi K, Hayashi N. A novel therapeutic approach for rectal varices: a case report of rectal varices treated with double balloon-occluded embolotherapy. *Am J Gastroenterol* 1997; **92**: 883-886
23 **Ota K**, Okazaki M, Higashihara H, Kokawa H, Shirai Z, Anan A, Kitamura Y, Shijo H. Combination of transileocolic vein obliteration and balloon-occluded retrograde transvenous obliteration is effective for ruptured duodenal varices. *J Gastroenterol* 1999; **34**: 694-699
24 **Kiyosue H**, Mori H, Matsumoto S, Yamada Y, Hori Y, Okino Y. Transcatheter obliteration of gastric varices: Part 2. Strategy and techniques based on hemodynamic features. *Radiographics* 2003; **23**: 921-937; discussion 937
25 **Greig JD**, Garden OJ, Anderson JR, Carter DC. Management of gastric variceal haemorrhage. *Br J Surg* 1990; **77**: 297-299

S- Editor Pan BR **L- Editor** Kumar M **E- Editor** Bai SH

The role of nuclear receptor CAR in the pathogenesis of non-alcoholic steatohepatitis.

Yuichi Yamazaki [1], Satoru Kakizaki [1], Norio Horiguchi [1], Naondo Sohara [1], Ken Sato [1], Hitoshi Takagi [1], Masatomo Mori [1], and Masahiko Negishi [2]

[1]Department of Medicine and Molecular Science, Gunma University Graduate School of Medicine, Maebashi, Gunma 371-8511, Japan;
[2]Pharmacogenetics Section, Laboratory of Reproductive and Developmental Toxicology, National Institute of Environmental Health Sciences, National Institutes of Health, Research Triangle Park, North Carolina 27709, USA.

Corresponding author:
Satoru Kakizaki, M.D., Ph.D.,
Department of Medicine and Molecular Science,
Gunma University Graduate School of Medicine,
3-39-15 Showa-machi, Maebashi, Gunma 371-8511, Japan.
Tel: +81-27-220-8127, Fax: +81-27-220-8136
E-mail: kakizaki@showa.gunma-u.ac.jp

Running title: Nuclear receptor CAR in the non-alcoholic steatohepatitis.

List of abbreviations:
CAR, constitutive androstane receptor; NASH, non-alcoholic steatohepatitis; CYP, cytochrome P450; MCD diet, methionine- and choline-deficient diet; TCPOBOP, 1,4 bis[2-(3,5-dichloropyridyloxy)]benzene; PB, phenobarbital; UGT, UDP-glucuronosyltransferase; MRP, multidrug resistance-associated protein ; RXR, retinoid X receptor; PXR, pregnane X receptor; PBREM, phenobarbital-responsive enhancer module; α-SMA, alpha-smooth muscle actin; iNOS, inducible nitric oxide synthase; TNF-α, tumor necrosis factor-α; TIMP-1, tissue inhibitor of metalloproteinase-1; MMP-13, matrix metalloproteinase-13; ROS, reactive oxygen species; 8-OHdG, 8-hydroxy-2'-deoxyguanosine; F2-isoprostane, 8-iso-Prostaglandin $F_{2\alpha}$

Key words: CAR; nuclear receptor; non-alcoholic steatohepatitis; cytochrome P450; methionine- and choline-deficient diet.

Abstract

Background; Non-alcoholic fatty liver disease is a common liver injury but the pathophysiological mechanisms leading to the development of non-alcoholic steatohepatitis (NASH) remain unclear. We investigated the pathological roles of nuclear receptor CAR, a key regulator of drug-metabolizing enzymes, in the development of NASH.

Methods and results; $CAR^{+/+}$ and $CAR^{-/-}$ mice were administered a methionine- and choline-deficient (MCD) diet to establish a dietary model of NASH. An elevation of the serum ALT and an increased infiltration of inflammatory cells were dominant in $CAR^{+/+}$ mice at 8 weeks. There was no significant difference in the liver lipid concentration, namely the first hit, between $CAR^{+/+}$ and $CAR^{-/-}$ mice. The index of lipid peroxidation increased in the liver of the $CAR^{+/+}$ mice which demonstrated by F2-isoprostanes. Western blotting analysis revealed that nuclear translocation of CAR occurred in $CAR^{+/+}$ mice fed the MCD diet. As a result, the CAR activation caused the lipid peroxidation, namely the second hit. The expressions of CYP2B10, 2C29, 3A11 all significantly increased in the $CAR^{+/+}$ mice. Furthermore, α-SMA immunohistochemistry and Sirius red staining revealed an increase in the degree of fibrosis in $CAR^{+/+}$ mice fed the MCD diet at 16 weeks. The mRNA expressions of collagen α1(1) and the tissue inhibitor of metalloproteinase-1 were found to be elevated in $CAR^{+/+}$ mice.

Conclusion; The receptor CAR caused the worsening of the hepatic injury and fibrosis in the dietary model of NASH. Our results suggest that nuclear receptor CAR may thus play a critical role in the pathogenesis of NASH.

Introduction

Nonalcoholic steatohepatitis (NASH) is a common liver injury in which the histopathological abnormalities mimic those of alcoholic steatohepatitis [1]. The histopathological features include steatosis, evidence of liver cell injury, a mixed inflammatory lobular infiltrate, and variable degrees of fibrosis [1-3]. The pathophysiological mechanisms leading to the development of NASH remain unclear [1-3]. A two-hit theory has been proposed, thus hepatic steatosis as the first hit and the triggering host or environmental factors as the second hit to precipitate a cascade of events leading to cell necrosis, inflammation, and fibrosis [4-6].

The nuclear receptor CAR (constitutive androstane receptor) is a key regulator of such xenobiotic-metabolizing enzymes as cytochrome P450 (CYP) [7-9], UDP-glucuronosyltransferase (UGT) [10, 11] and multidrug resistance-associated protein (MRP) [12, 13]. The receptor CAR, which acts as a heterodimer with the retinoid X receptor (RXR), binds to a nuclear receptor-binding site NR1 within the 51-bp PBREM (phenobarbital-responsive enhancer module) thereby activating the xenobiotic-metabolizing enzymes genes [7-9]. The receptor CAR is known to up-regulate CYP2B and 3A, which are considered to play an important role in drug-metabolizing. As a second hit, the environmental exposure to hepatotoxins has recently been implicated in NASH [14]. Furthermore, some chemicals have been known to clinically induce NASH, thus drug-induced NASH. Because of its nature as a xenobiotic sensor for environmental pollutions or drugs, CAR may play a role in the CYPs associated with NASH. Some other nuclear receptors such as PPAR-α and PPAR-γ are well known to be involved in the pathogenesis of NASH [15, 16].

As a result, the nuclear receptor may play a critical role in the pathogenesis of NASH because of its nature to regulate genes. Especially, nuclear receptors which regulate drug- or xenobiotic-metabolizing enzymes may also play a pathological role in the development of NASH. However, the precise relationship between CAR and NASH is still not fully understood. In this study, we investigated and revealed the pathogenesis of the receptor CAR in the development of NASH using CAR null mice who received a methionine- and choline-deficient (MCD) diet.

Materials and Methods

Materials

1, 4 bis[2-(3, 5-dichloropyridyloxy)]benzene (TCPOBOP) were purchased from Sigma Chemicals Co. (St. Louis, MO). The methionine- and choline-deficient (MCD) diet and control diets were both purchased from Funabashi Farm. (Chiba, Japan). All other chemicals were obtained from commercial sources at the highest grade of purity available.

Animals and treatment

The $CAR^{+/+}$ and $CAR^{-/-}$ mice used in this study were generated as described previously [17]. All mouse procedures were performed in accordance with the guidelines for animal care and use established by Gunma University Graduate School of Medicine. Germline transmission of the disrupted allele was detected by PCR [18]. Mice from each genotype were randomly divided into experimental groups and fed either a plain MCD diet or an MCD diet supplemented with choline bitartrate (2 g/kg) and DL-methionine (3 g/kg); the latter was designated as a control diet. A schematic presentation of the treatment protocol is shown in Figure 1. During the experimental period, the individual body weights and food intake were recorded 3 times per week. Male mice were fed an experimental diet at 5 to 6 weeks of age and were then sacrificed, and their sera and livers were collected after 8 or 16 weeks of feeding (n = 6 per treatment group). The each experiment was performed independently at least 3 times. To activate the CAR, TCPOBOP was administered twice a week in olive oil at a dose of 3 mg/kg body weight from 6 to 8 weeks of feeding. In the control mice, 100 μl of olive oil per 25 g of body weight was injected. The serum alanine aminotransferase (ALT), total bilirubin, blood urea nitrogen (BUN), triglyceride (TG) and total cholesterol (T-Cho) levels were all measured with an auto-analyzer. For the histological examinations, liver tissue specimens were fixed in 10% formalin, embedded in paraffin and then stained with hematoxylin-eosin. Blinded investigators (NS and KS) evaluated the slides and assigned a score for steatosis and inflammation as follows: steatosis—grade 0, none present; grade 1, steatosis of <25% of parenchyma; grade 2, steatosis of 26–50% of parenchyma; grade 3, steatosis 51–75% of parenchyma; grade 4, steatosis >76% of parenchyma. For inflammation—grade 0, no inflammatory foci; grade 1, <5 inflammatory foci/hpf; grade 2, >5 inflammatory foci/hpf. An immunohistochemical analysis for 8-hydroxy-2'-deoxyguanosine (8-OHdG), nitrotyrosine, nuclear factor-kappaB (NF-kappaB), and alpha-smooth muscle actin (α-SMA) was performed by the avidin-biotin-peroxidase complex (ABC) method (Vectastain ABC kit, Vector Laboratories Inc., Burlingame, CA) using anti-8-OHdG (CHEMICON International, Inc., Temecula, CA), nitrotyrosine (CHEMICON International, Inc.), NF-kappaB (Santa Cruz Biotechnology, Santa Cruz, CA), α -SMA (DAKO, Glostrup, Denmark) antibodies. The sites of peroxidase binding were determined using the diaminobenzidine method. At a magnification of x200, 10 areas of α-SMA positive cells were measured in a blinded fashion for each group. Sirius red staining was performed according to the usual method and the area of the Sirius red positive area was measured using the NIH image software program (National

Institute of Health, MD) in nine microscopic fields at a 200-fold magnification and the mean ± SD were thus shown.

Reverse transcription-polymerase chain reaction

Total RNA extraction from the liver and the subsequent synthesis of first strand cDNA were performed using TRIzol reagent (Invitrogen, Carlsbad, CA) and the SuperScript™ preamplification system (Invitrogen), respectively. cDNAs were amplified using the following sets of primers: CYP1A2 mRNA, 5'-CCAAGGAGCGCTGTATC-3' and 5'-AAGCCGAAGAGCATCAC-3'; CYP2A5 mRNA, 5'-CTCTTCTTTGCTGGCACA-3' and 5'-TCCGTATAGGGCATCTTCATT-3'; CYP2B10 mRNA, 5'-CACCACGCTCCACTATGGCT-3' and 5'-CTGTGTGGCACTCCAATAGGTATAA-3'; CYP2D9 mRNA, 5'-ATTCCCGATACTCTTGCG-3' and 5'-CAGGAAGGCATCAGTCAAA-3'; CYP2E1, 5'-CCCAGGACCTTTCCCAATTC-3' and 5'-TGACCCAGGTGCAGTGTGAA-3'; CYP2C29 mRNA, 5'-AAACAGGTAAACCACATTGAAC-3' and 5'-GTCAATCTCTTCCTGGACTTTAG-3'; CYP3A11 mRNA, 5'-GGGTGCTCCTAGCAATCAGCT-3' and 5'-GTGCCTAAAAATGGCAGAGGTT-3', CYP4A10, 5'-GTGCTGAGGTGGACACATTCAT-3' and 5'-TGTGGCCAGAGCATAGAAGATC-3'; inducible nitric oxide synthase (iNOS), 5'-GAGATTGGAGGCCTTGTG-3' and 5'-TCAAGCACCTCCAGGAACGT-3'; tumor necrosis factor-α (TNF-α), 5'-CTGTGAAGGGAATGGGTGTT-3' and 5'-GGGGGCTCTGAGGAGTAGAC-3'; tissue inhibitor of metalloproteinase-1 (TIMP-1), 5'-CATGGAAAGCCTCTGTGGATATG-3' and 5'-GATGTGCAAATTTCCGTTCCTT-3'; collagen α1(1), 5'-CCTCAGGGTATTGCTGGACAAC-3' and 5'-ACCACTTGATCCAGAAGGACCTT-3'; matrix metalloproteinase-13 (MMP-13), 5'-ACTTAACTTACAGGATTGTGAACTATACTCCT-3' and 5'-TGTCAGCAGTGCCATCATAGATT-3'. One-twentieth of each cDNA synthesized from 5 μg of RNA was subjected to real time PCR using SYBR green dye (PE Applied Biosystems, Foster City, CA).

Hepatic lipid concentration and lipid peroxidation

Total liver lipids were extracted from 50 mg of liver homogenate using methanol and chloroform, and then were followed by a reaction with a vanillin-phosphoric acid reagent [19]. The total triglycerides were determined using the triglyceride GPO-Trinder kit (Sigma-Aldrich, St. Louis, MO).

To determine an index of lipid peroxidation, 8-iso-Prostaglandin F2□ (F2-isoprostane) were measured in 100 mg liver homogenate using the Direct 8-iso-Prostaglandin $F_{2\alpha}$ Enzyme Immunoassay Kit (Assay Designs, Inc., Ann Arbor, MI) following the manufacturer's instructions.

Western blotting analysis

Nuclear extracts were resolved on a sodium dodecyl sulfate (SDS)-10% polyacrylamide gel, transferred to a polyvinylidene difluoride (PVDF) membrane, and incubated with anti-CAR antibody (Santa Cruz Biotechnology). Microsome extracts

were also resolved on a 10%-SDS polyacrylamide gel, transferred to a PVDF membrane, and incubated with anti-CYP2B1, CYP2C6, CYP3A2 (Daiichi Pure Chemicals Co., Ltd.,Tokyo, Japan), CYP2E1 (BIOMOL International, LP, Plymouth meeting, PA) antibodies. After incubation with the secondary antibodies, the immunoreactive bands were visualized using an enhanced chemiluminescence system (Amersham, Buckinghamshire, UK).

Data analysis

All experimental data are shown as the means $\pm$ SD. The differences were determined by a one-way factorial analysis of variance (ANOVA) for each group. The level of significance for all statistical analyses was set at $P<0.05$.

Results

Body and liver weights of the mice.

The mice fed the MCD diet lost weight in comparison to the animals fed the control diet in both $CAR^{+/+}$ and $CAR^{-/-}$ mice (Table 1) consistent with the findings of a previous study [6], despite a higher food intake relative to their body weight. Despite the extent of weight loss, the general condition of the animals remained good and their behavior appeared normal throughout the experimental period. There was no difference in the body weight between the $CAR^{+/+}$ and $CAR^{-/-}$ mice fed the MCD diet for 8 weeks. Although there was no difference in the body weight between the $CAR^{+/+}$ and $CAR^{-/-}$ mice fed the MCD diet, relative liver weight (liver weight/body weight) was significantly elevated in $CAR^{+/+}$ mice in comparison to the $CAR^{-/-}$ mice (Table 1). As a result, the livers of the $CAR^{+/+}$ mice fed the MCD diet were significantly larger than the livers of the $CAR^{-/-}$ mice.

Table 1. The body weight, relative liver weight, and serum and hepatic lipids in $CAR^{+/+}$ and $CAR^{-/-}$ mice fed the methionine- and choline-deficient (MCD) or control diet for 8 weeks.

	$CAR^{+/+}$		$CAR^{-/-}$	
	Control	MCD	Control	MCD
Body weight (g)	31.0±1.4	24.4±1.7**	29.6±1.6	25.6±1.5**
Relative liver weight (%)	4.5±0.4	11.7±2.5**	4.4±0.3	8.2±0.6**, †
Serum triglyceride (mg/dl)	124±35	63±18*	124±77	55±22**
Hepatic triglyceride (mg/g wet liver)	76±18	270±27*	56±25	286±27*

*; $P< 0.05$, **; $P< 0.01$ in comparison to control diet, †; $P< 0.01$ in comparison to $CAR^{+/+}$ mice. Data are mean ± SD.

Serum alanine aminotransferase level and histological change with the MCD diet.

Consumption of the MCD diet resulted in a major increase in the serum ALT levels in comparison to the controls after receiving this dietary regimen for 8 weeks (Figure 2A). This elevation in the ALT level was significantly dominant in the $CAR^{+/+}$ mice in comparison to $CAR^{-/-}$ mice. The administration of TCPOBOP, CAR agonist significantly elevated the ALT level in the $CAR^{+/+}$ mice but not in the $CAR^{-/-}$ mice (Figure 2A). Hematoxylin and eosin histological slides were evaluated by blinded investigators and analyzed using a semi-quantitative score for steatosis and inflammation. Consistent with serum ALT levels, inflammatory cell infiltration and hepatocyte necrosis dissecting the liver parenchyma in the $CAR^{+/+}$ mice were more severe than in the $CAR^{-/-}$ mice (Figure 2B). Inflammation score for the $CAR^{-/-}$ mice was lower than the $CAR^{+/+}$ mice (0.8±0.3 vs. 1.7±0.3, $P<0.01$). Both the $CAR^{+/+}$ and $CAR^{-/-}$ mice fed the MCD diet had significant steatosis compared to the mice fed the control diet. The livers revealed lipid droplets as clear macrovacuoles affecting all but zone 1 hepatocytes (periportal hepatocytes) (Figure 2B). Staining with oil red O confirmed the lipid content of these vacuoles (data not shown). There were no significant changes in steatosis score between the $CAR^{+/+}$ and $CAR^{-/-}$ mice fed the MCD diet (2.3±0.2 vs. 2.2±0.3).

Lipid content and lipid peroxidation in the liver.

The lipid contents of the liver are shown in Table 1. Consistent with the morphological changes of lipid depositions, the total hepatic lipid content increased in the MCD diet in comparison with the control diet (Table 1). The concentrations of triglyceride increased 3-fold in the liver prepared from the MCD diet-fed mice in comparison to the control diet. However, there was no significant change between the $CAR^{+/+}$ mice and $CAR^{-/-}$ mice regarding the hepatic triglyceride levels fed the MCD diet. As a result, there was no difference in the first hit between the $CAR^{+/+}$ mice and $CAR^{-/-}$ mice.

The index of lipid peroxidation, namely the F2-isoprostane, increased 3-fold in the liver prepared from the MCD diet-fed mice in comparison to the controls in the $CAR^{+/+}$ mice after 8 weeks of treatment. The F2-isoprostane significantly increased in the $CAR^{+/+}$ mice fed the MCD diet in comparison to the $CAR^{-/-}$ mice fed the MCD diet (Figure 3A). Immunohistochemistry for 8-OHdG, an index of oxidative DNA damage, showed an increased accumulation in the nuclei of the hepatocytes in the $CAR^{+/+}$ mice in comparison to the $CAR^{-/-}$ mice (Figure 3B).

Nuclear translocation of CAR with MCD diet.

It is well known that the first step of induction of CYPs is translocation of CAR into nuclei. To evaluate the nuclear translocation of CAR, the nuclear extracts were subjected to Western blotting analysis. Nuclear content of CAR increased in $CAR^{+/+}$ mice fed the MCD diet for 8 weeks (Figure 4A). Thus, CAR activation step occurred in $CAR^{+/+}$ mice fed the MCD diet.

Hepatic gene and protein expressions in CAR+/+ and CAR-/- mice fed MCD diet.

To characterize the hepatic gene expression related to NASH in $CAR^{+/+}$ and $CAR^{-/-}$ mice fed the MCD or control diet, we determined the levels of liver CYPs, iNOS and TNF-α mRNA levels. As a result, no differences were observed in the CYP2E1, CYP2D9 and CYP4A10 expressions between the $CAR^{+/+}$ and $CAR^{-/-}$ mice fed the MCD diet (Figure 4B). The mRNA expression of CYP2B10, CYP2C29 and CYP3A11 increased in the $CAR^{+/+}$ mice fed the MCD diet in comparison to the $CAR^{-/-}$ mice. The mRNA expression of CYP1A2 and CYP2A5 decreased in the $CAR^{-/-}$ mice in comparison to the $CAR^{+/+}$ mice, although the differences were smaller than those of CYP2B10, CYP2C29 and CYP3A11. Furthermore, the protein levels of CYP2B10, CYP2C29, CYP3A11 and CYP2E1 were also determined by Western blotting (Figure 4C). The protein levels of CYP2B10, CYP2Cs and CYP3As increased in the $CAR^{+/+}$ mice fed the MCD diet in comparison to the $CAR^{-/-}$ mice. In addition, no significant change was seen in the protein levels of the CYP2E1 expression between the $CAR^{+/+}$ and $CAR^{-/-}$ mice.

The promoter region of iNOS, one of the second hit candidates of NASH, have nuclear receptor binding sites including CAR/RXR and PXR/RXR [20]. The mRNA expression of iNOS was repressed in the $CAR^{-/-}$ mice in comparison with the $CAR^{+/+}$ fed the MCD diet (Figure 5A). Furthermore, immunohistochemistry for nytrotyrosine showed an increased amount of protein nytrosylation in the $CAR^{+/+}$ mice in comparison to the $CAR^{-/-}$ mice (Figure 5B). The mRNA expression of TNF-α was

slightly repressed in the $CAR^{-/-}$ mice in comparison with $CAR^{+/+}$ fed the MCD diet (Figure 5A), although it did not reach statistical significance. Since NF-kappaB is activated in the presence of proinflammatory stimuli, and its activation results in an increased expression of various proinflammatory and immune response genes including TNF-α, immunohistochemistry for NF-kappaB was performed. It showed increased nuclear and cytosolic expressions of activated NF-kappaB in the $CAR^{+/+}$ mice fed the MCD diet (Figure 5C).

Long term treatment with the MCD diet caused hepatic fibrosis and an elevation in the mRNA expression of the gene related to liver fibrosis.

To evaluate the effect of CAR on hepatic fibrosis in a NASH model with MCD diet, long term effect of MCD diet was evaluated in $CAR^{+/+}$ and $CAR^{-/-}$ mice. At 16 weeks after consuming the MCD diet, both perivenular and pericellular fibrosis was more clearly observed in the $CAR^{+/+}$ mice than in the $CAR^{-/-}$ mice. Sirius red (Figure 6A, 6B) and immunohistochemistry for α-SMA (Figure 6C, 6D) showed an increase in the fibrotic changes in the $CAR^{+/+}$ mice in compared to the $CAR^{-/-}$ mice. Furthermore, the mRNA expressions of fibrogenic markers, collagen α1(1) and TIMP-1 were significantly elevated in the $CAR^{+/+}$ mice in comparison to the $CAR^{-/-}$ mice (Figure 7). There was no difference in the mRNA expression of the anti-fibrogenic marker MMP-13 between the $CAR^{+/+}$ mice and the $CAR^{-/-}$ mice (Figure 7).

Discussion

In this study, we showed that CAR worsened the dietary model of NASH with the MCD diet, associated with an elevation in the lipid peroxidation and the induction of CYPs and iNOS. There was also no change in the lipid concentration of the liver between the $CAR^{+/+}$ and $CAR^{-/-}$ mice. As a result, there was no change in the first hit. Lipid peroxidation caused the inflammation to develop into NASH. Furthermore, the long term treatment caused an elevation of the fibrogenic gene expression and fibrosis. Although a study by Leclercq *et al.* [6] showed an elevation of CYP2E1 mRNA and protein, and indicated CYP2E1 played a major role in the MCD diet NASH model, there were no significant differences in the CYP2E1 and CYP4A expression between the $CAR^{+/+}$ and $CAR^{-/-}$ mice in our study. In comparison to the findings of their study, the development of NASH with MCD diet occurred more slowly in this strain of mice (C3H). CYPs are well known to have species or sex differences. Such species or sex differences may thus have caused the differences between our study (C3H male mice) and their study (C57BL6/J female mice). CYP2E1 has been proposed to be a potential inducer of lipid peroxidation in NASH since its expression and activity have been shown to be up-regulated in rat and mouse models of NASH [6, 21, 22] as well as in humans [23, 24]. However, Leclercq *et al.* [6] showed that the development of experimental NASH could not be prevented in CYP2E1 knockout mice. They suggested that hepatic CYP4A might be a source of lipid peroxidation and a substitute for CYP2E1 if the latter is absent [6]. As a result, CYPs have low substrate specificities and other CYPs may be substituted for repressed CYP. Not only CYP2E1 but also CYP1A, CYP2B and CYP3A have been reported to be induced by alcoholic hepatitis [25]. Kono *et al.* [25] showed that CYP2B and CYP3A both produce reactive oxygen species (ROS) which thus causes alcoholic hepatitis, while CYP2E1 plays only a small role in the mechanism of early alcoholic liver injury. As a result, many CYPs other than CYP2E1 are also related to NASH or alcoholic hepatitis. Although one of the CYPs related to NASH was knocked out in mice, the CYPs network can be substituted for repressed CYP. CYPs network is closely associated with each other and thus overlaps with the substrates. Therefore, nuclear receptors regulating CYPs seem to play an important role in the pathogenesis of NASH.

Nuclear receptors PPAR-α and PPAR-γ have been reported to be involved in the pathogenesis of NASH [15, 16]. CAR also belongs to the nuclear receptor superfamilies forming a heterodimer with RXR in the same manner as PPAR-α and PPAR-γ. PPAR-α is highly expressed in the liver and its activation by agonists leads to augmented fatty acid oxidation while also protecting against steatosis. PPAR-γ, which is transcriptionally up-regulated in steatosis, activates lipogenic enzymes and exacerbates steatosis. However, the roles of these nuclear receptors in the pathogenesis in NASH are more complicated and are not simple to understand. Ip *et al.* [26] recently showed that the massive induction of CYP4A after the administration of a PPAR-α agonist in MCD mice did not lead to an increased lipid peroxidation. Interestingly, in the study by Ip *et al.*, the pretreatment of MCD mice with a PPAR-α agonist not only induced CYP4A but also prevented the occurrence of steatosis [26, 27]. As a result, CYPs or lipid metabolizing enzymes are closely associated with each other while also interacting with each other. To understand these networks of CYPs

and the lipid metabolic enzymes regulated by nuclear receptors is thus considered to be one way to reveal the pathogenesis of NASH.

Human beings are exposure to various types of environmental pollution or drugs throughout their lifetime. Environmental pollution or drugs are one of the causes of NASH [14], and they are potent inducers of nuclear receptor CAR and CYPs. In our study, the MCD diet caused an elevation in the ALT levels in the $CAR^{+/+}$ mice in comparison to the $CAR^{-/-}$ mice without a CAR inducer. Environmental stimulation may also cause the up regulation of CAR, due to the constitutively active nature of CAR. If environmental pollution or drugs cause NASH, then an inverse agonist of CAR, such as androstanol, may be a potentially effective treatment strategy for NASH.

In this study, the short-term administration of CAR agonist, TCPOBOP caused the severe liver injury in the $CAR^{+/+}$ mice fed the MCD diet. TCPOBOP itself did not have any toxicity in the mice fed the control diet. Treatment with the MCD diet resulted in the nuclear translocation of CAR while also increasing the expression of CAR target genes in the $CAR^{+/+}$ mice. The administration of TCPOBOP enhanced this phenomenon more clearly. Preliminarily, we also tried to evaluate the parameters of liver fibrosis with long-term administration of TCPOBOP. However, the CAR activation with TCPOBOP caused the marked liver enlargement in the $CAR^{+/+}$ mice. As shown in Table 1, MCD diet itself caused the liver enlargement in the both mice, more prominent in the $CAR^{+/+}$ mice. We tried to intraperitoneally inject the same dosage of TCPOBOP with this experiment for several weeks. However, the marked liver enlargement in the $CAR^{+/+}$ mice fed MCD diet prevented us from continuing the injections long term to evaluate the fibrosis. Because TCPOBOP enhanced the liver injury after short-term administration, we thus think that the long term administration of a small amount of TCPOBOP may worsen the degree of liver fibrosis as a result of liver injury.

CAR is known not only as a CYP regulating receptor, but also as a regulator of many other enzymes [18]. Since the iNOS-induced production of nitric oxide is known to influence inflammation and apoptosis, iNOS is therefore considered to play a role in the pathogenesis of NASH. In addition, CAR/RXR and PXR/RXR binding sites have also reported in the promoter region of the human iNOS gene [20]. In the natural iNOS promoter context, the DR4-type response element specifically mediates the down-regulation of the promoter activity by androstanol through CAR/RXR heterodimers and the up-regulation by the xenobiotic drug clotrimazole through PXR/RXR heterodimers [20]. In our study, iNOS was induced with the MCD diet to a greater content than in the controls, and it was also elevated in $CAR^{+/+}$ mice in comparison to the level in $CAR^{-/-}$ mice fed the MCD diet. CAR and PXR have a rather broad, overlapping set of ligands and they also recognize similar DNA binding sites in the promoter regions of regulating genes. Because PXR is also a key-regulator of the CYPs and drug metabolizing enzymes, PXR may also contribute to the pathogenesis of NASH. Although PXR null or CAR/PXR double null mice were not available for this study, further studies using PXR null mice should provide us with valuable insight into the precise understanding of the pathogenesis of NASH.

In conclusion, the nuclear receptor CAR worsened the dietary model of NASH inducing lipid peroxidation. Our results suggest that the nuclear receptor CAR may

thus play a critical role in the pathogenesis of NASH. Further study evaluating the role of CAR and PXR in NASH is thus called for in the future.

Grant support:
This work was supported in part by a Grant-in Aid for Scientific Research (No.18590716) from the Ministry of Education, Science, Sports and Culture of the Japanese Government.

Competing Interest: None declared.

Figure Legends

Figure 1. Treatment protocol.

Figure 2. The ALT elevation and inflammatory cell infiltration with the methionine- and choline-deficient (MCD) diet for 8 weeks. (A) The ALT levels. TCPOBOP was administered as described in the materials and methods. The data are the mean ± SD. *; $P< 0.01$ in comparison to control diet, #; $P< 0.01$ in comparison between $CAR^{+/+}$ and $CAR^{-/-}$ mice, ‡; $P< 0.05$ in comparison to MCD diet without TCPOBOP. (B) The histological findings in the liver (hematoxylin and eosin staining); a, $CAR^{+/+}$ mice, control diet; b, $CAR^{-/-}$ mice, control diet; c, $CAR^{+/+}$ mice, MCD diet; d, $CAR^{-/-}$ mice, MCD diet. The administration of the MCD diet to both groups produced severe macrovesicular and panlobular steatosis. The infiltration of the inflammatory cells and hepatic necrosis was more prominent in the $CAR^{+/+}$ liver than the $CAR^{-/-}$ mice. The arrows indicate the inflammatory cells infiltrations. V; Central vein. Magnification, x 400.

Figure 3. (A) An index of lipid peroxidation measured with F2-isoprostane in the liver samples treated with each diet for 8 weeks. The data are the means ± SD. *; $P< 0.01$ in comparison to control diet, #; $P< 0.01$ in comparison between $CAR^{+/+}$ and $CAR^{-/-}$ mice. (B) 8-hydroxy-2'-deoxyguanosine (8-OHdG) staining. a, $CAR^{+/+}$ mice, control diet; b, $CAR^{-/-}$ mice, control diet; c, $CAR^{+/+}$ mice, MCD diet; d, $CAR^{-/-}$ mice, MCD diet. The arrows indicate the positive staining of 8-OHdG to the nuclei. Magnification, x 400.

Figure 4. Nuclear translocation of CAR and hepatic mRNA and protein levels fed the MCD diet or the control diet for 8 weeks. (A) Western blotting analysis of nuclear CAR. Nuclear extracts were prepared and subjected to an analysis with anti-CAR antibody as indicated in the materials and methods. (B) mRNA expression of CYPs. Total liver RNA was prepared from $CAR^{+/+}$ or $CAR^{-/-}$ mice and subjected to a real-time PCR analysis with the indicated primers in the materials and methods. *; $P< 0.01$ in comparison to control diet, #; $P< 0.01$ in comparison between $CAR^{+/+}$ and $CAR^{-/-}$ mice. (C) The CYP2B, CYP2C, CYP3A and CYP2E protein expression. Microsome extracts were prepared from the liver and then were subjected to a Western blotting analysis as described in the materials and methods. The arrow indicates the corresponding band for CYP2B10.

Figure 5. (A) mRNA expression of iNOS and TNF-α. *; $P< 0.01$ in comparison to control diet, #; $P< 0.01$ in comparison between $CAR^{+/+}$ and $CAR^{-/-}$ mice. (B) Nitrotyrosine staining. a, $CAR^{+/+}$ mice, cotrol diet; b, $CAR^{-/-}$ mice, control diet; c, $CAR^{+/+}$ mice, MCD diet; d, $CAR^{-/-}$ mice, MCD diet. Magnification, x 400. (C) Nuclear factor-kappaB staining. a, $CAR^{+/+}$ mice, control diet; b, $CAR^{-/-}$ mice, control diet; c, $CAR^{+/+}$ mice, MCD diet; d, $CAR^{-/-}$ mice, MCD diet. Magnification, x 200.

Figure 6. Long term treatment with MCD diet for 16 weeks. (A) Sirius red staining. a, $CAR^{+/+}$ mice, control diet; b, $CAR^{-/-}$ mice, control diet; c, $CAR^{+/+}$ mice, MCD diet; d, $CAR^{-/-}$ mice, MCD diet. (B) The quantification of Sirius red positive areas using the NIH image software program. Nine microscopic fields at a 200-fold magnification were measured and the means ± SD are shown. *; $P< 0.01$ in comparison to control diet, #; $P< 0.01$ in comparison between $CAR^{+/+}$ and $CAR^{-/-}$ mice. (C) Alpha smooth muscle actin (α-SMA) staining. a, $CAR^{+/+}$ mice, control diet; b, $CAR^{-/-}$ mice, control diet; c, $CAR^{+/+}$ mice, MCD diet; d, $CAR^{-/-}$ mice, MCD diet. (D) The number of α-SMA positive cells. Ten areas of α-SMA positive cells were counted at 200-fold magnification and the means ± SD are shown. Magnification, x 200. *; $P< 0.01$ in comparison to control diet, #; $P< 0.01$ in comparison between $CAR^{+/+}$ and $CAR^{-/-}$ mice.

Figure 7. Hepatic mRNA expressions relating to fibrosis. Total liver RNA was prepared from $CAR^{+/+}$ or $CAR^{-/-}$ mice treated with each diet for 16 weeks, and then were subjected to a real-time PCR analysis with the indicated primers in the materials and methods. The fold induction of the mRNA level from the $CAR^{+/+}$ mice fed the control diet was indicated. *; $P< 0.01$ in comparison to control diet, #; $P< 0.01$ in comparison between $CAR^{+/+}$ and $CAR^{-/-}$ mice.

References

1. Ludwig J, Viggiano TR, McGill DB, et al. Nonalcoholic steatohepatitis: Mayo Clinic experiences with a hitherto unnamed disease. *Mayo Clin Proc.* 1980;55:434-8.
2. Diehl AM, Goodman Z, Ishak KG. Alcohollike liver disease in nonalcoholics. A clinical and histologic comparison with alcohol-induced liver injury. *Gastroenterology.* 1988;95:1056-62.
3. Powell EE, Cooksley WG, Hanson R, et al. The natural history of nonalcoholic steatohepatitis: a follow-up study of forty-two patients for up to 21 years. *Hepatology.* 1990;11:74-80.
4. Mehta K, Van Thiel DH, Shah N, et al. Nonalcoholic fatty liver disease: pathogenesis and the role of antioxidants. *Nutr Rev.* 2002;60:289-93.
5. Sass DA, Chang P, Chopra KB. Nonalcoholic fatty liver disease: a clinical review. *Dig Dis Sci.* 2005;50: 171-80.
6. Leclercq IA, Farrell GC, Field J, et al. CYP2E1 and CYP4A as microsomal catalysts of lipid peroxides in murine nonalcoholic steatohepatitis. *J Clin Invest.* 200;105:1067-75.
7. Honkakoski P, Moore R, Washburn K, et al. Activation by diverse xenochemicals of the 51-base pair phenobarbital-responsive enhancer module in the CYP2B10 gene. *Mol Pharmacol* 1998;**53**:597-601
8. Honkakoski P, Zelko I, Sueyoshi T, et al. The nuclear orphan receptor CAR-retinoid X receptor heterodimer activates the phenobarbital-responsive enhancer module of the CYP2B gene. *Mol Cell Biol* 1998;**18**:5652-5658
9. Sueyoshi T, Kawamoto T, Zelko I, et al. The repressed nuclear receptor CAR responds to phenobarbital in activating the human CYP2B6 gene. *J Biol Chem* 1999;**274**:6043-6046
10. Sugatani J, Kojima H, Ueda A, et al. The phenobarbital response enhancer module in the human bilirubin UDP-glucuronosyltransferase UGT1A1 gene and regulation by the nuclear receptor CAR. *Hepatology* 2001; **33**:1232-8.
11. Xie W, Yeuh MF, Radominska-Pandya A, et al. Control of steroid, heme, and carcinogen metabolism by nuclear pregnane X receptor and constitutive androstane receptor. *Proc Natl Acad Sci USA* 2003; **100**:4150-5.
12. Kast HR, Goodwin B, Tarr PT, et al. Regulation of multidrug resistance-associated protein 2 (ABCC2) by the nuclear receptors pregnane X receptor, farnesoid X-activated receptor, and constitutive androstane receptor. *J Biol Chem* 2002; **277**: 2908-15.
13. Cherrington NJ, Hartley DP, Li N, et al. Organ distribution of multidrug resistance proteins 1, 2, and 3 (Mrp1, 2, and 3) mRNA and hepatic induction of Mrp3 by constitutive androstane receptor activators in rats. *J Pharmacol Exp Ther* 2002; **300**: 97-104.
14. Cotrim HP, Andrade ZA, Parana R, et al. Nonalcoholic steatohepatitis: a toxic liver disease in industrial workers. *Liver.* 1999;**19**:299-304.
15. Chitturi S, Farrell GC. Etiopathogenesis of nonalcoholic steatohepatitis. *Semin Liver Dis.* 2001;**21**:27-41.

16. Neuschwander-Tetri BA, Brunt EM, Wehmeier KR, et al. Improved nonalcoholic steatohepatitis after 48 weeks of treatment with the PPAR-gamma ligand rosiglitazone. *Hepatology.* 2003;**38**:1008-17.
17. Yamamoto Y, Moore R, Goldsworthy TL, et al. The orphan nuclear receptor CAR is essential for liver tumor promotion by phenobarbital in mice. *Cancer Res.* 2004;**64**:7197-200
18. Ueda A, Hamadeh HK, Webb HK, et al. Diverse roles of the nuclear orphan receptor CAR in regulating hepatic genes in response to phenobarbital. *Mol Pharmacol* 2002; **61**: 1-6.
19. Folch J, Less M, Sloane Stanley GH. A simple method for the isolation and purification of total lipides from animal tissues. *J Biol Chem.* 1957;**226**:497-509.
20. Toell A, Kroncke KD, Kleinert H, et al. Orphan nuclear receptor binding site in the human inducible nitric oxide synthase promoter mediates responsiveness to steroid and xenobiotic ligands. *J Cell Biochem.* 2002;**85**:72-82.
21. Lieber CS, Leo MA, Mak KM, et al. Model of nonalcoholic steatohepatitis. *Am J Clin Nutr.* 2004;**79**:502-9.
22. Weltman MD, Farrell GC, Liddle C. Increased hepatocyte CYP2E1 expression in a rat nutritional model of hepatic steatosis with inflammation. *Gastroenterology.* 1996;**111**:1645-53.
23. Weltman MD, Farrell GC, Hall P, et al. Hepatic cytochrome P450 2E1 is increased in patients with nonalcoholic steatohepatitis. *Hepatology.* 1998;**27**:128-33.
24. Chalasani N, Gorski JC, Asghar MS, et al. Hepatic cytochrome P450 2E1 activity in nondiabetic patients with nonalcoholic steatohepatitis. *Hepatology.* 2003;**37**:544-50.
25. Kono H, Bradford BU, Yin M, et al. CYP2E1 is not involved in early alcohol-induced liver injury. *Am J Physiol.* 1999;**277**:G1259-67.
26. Ip E, Farrell GC, Robertson G, et al. Central role of PPARalpha-dependent hepatic lipid turnover in dietary steatohepatitis in mice. *Hepatology.* 2003;**38**:123-32.
27. Ip E, Farrell G, Hall P, et al. Administration of the potent PPARalpha agonist, Wy-14,643, reverses nutritional fibrosis and steatohepatitis in mice. *Hepatology.* 2004;**39**:1286-96.